A study of friction models and friction compensation

V. van Geffen

DCT 2009.118

Traineeship report

Coach(es): Ir. D.J. Rijlaarsdam
Dr. ir. P.W.J.M. Nuij

Supervisor: Prof. dr. ir. M. Steinbuch

Technische Universiteit Eindhoven
Department Mechanical Engineering
Dynamics and Control Technology Group

Eindhoven, December, 2009

Contents

Introduction

Friction is generally described as the resistance to motion when two surfaces slide against each other. In most cases friction is a useful phenomena making many ordinary things like walking and the brake in a car possible. On the other hand friction can also cause undesirable effects. For high precision mechanical motion systems for example, friction can deteriorate the performance of the system. Possible unwanted consequences caused by friction are steady-state errors, limit cycling and hunting. In motion control a possible way to minimize the influences of friction is to compensate for it. In order to be able to compensate the effect of friction, it is necessary to describe the frictional behavior. Since no exact formula for the friction force is available, friction is normally described in an empiric model. By canceling the friction effect, the nonlinearity in the system, assuming no other nonlinear behavior is present, is removed. This is beneficial for classic control which is based on linearity and where the feedback is therefore not able to completely compensate for frictional effects.
The main purpose of this literature study is to gain more insight into the available friction models and their differences. Furthermore, different applications of friction compensation in motion control are studied.
Chapter 1 discusses different friction models found in literature. Static friction models are discussed first which are solely dependent on the velocity. For some applications that operate near zero velocity or cross zero velocity often, the static models do not describe friction accurately enough. For these situations a dynamic model is necessary which introduces an extra state which can be regarded as the average deflection of the asperities. Besides these dynamic models, physics-based model are briefly discussed in this chapter as well.
In chapter 2, different ways of friction compensation are described. A distinction is made between model-based and non model-based friction compensation. Furthermore friction compensation in feedforward and feedback is discussed. Other variations and combinations with adaptive control and observers for example are considered as well.

Chapter 1

Friction models

1.1 Static friction models

The most basic friction models contain Coulomb friction and linear viscous damping. For situations where the starting friction is higher than friction at a nonzero velocity "static" friction force F_s can be distinguished as can be seen in figure 1.1 (a). For the most common situations the friction decreases with increasing velocity for a certain velocity regime. This is called the Stribeck effect and is shown in figure 1.1 (b). These basic models describe a static relationship between the friction force and velocity. At rest where the velocity is zero, the friction force cannot be described as a function of velocity alone. The discontinuity at zero velocity also may lead to numerical difficulties which will not be discussed here in further detail. For some applications this static model is adequate enough to describe the effects of friction. For practical high accurate positioning systems however other frictional properties have to be considered for a satisfying model.

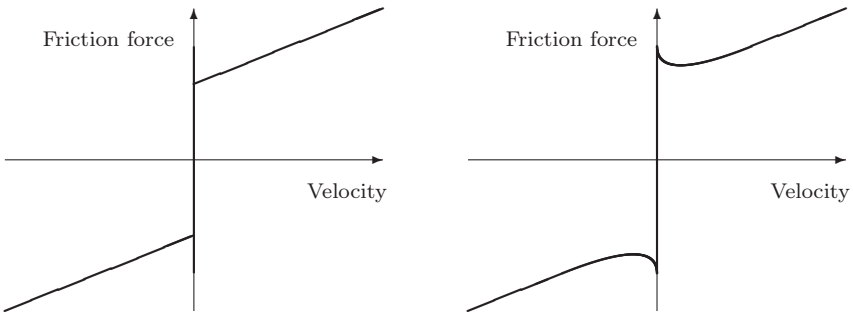

Figure 1.1: A global representation of the basic static friction force effects versus velocity. (a): Coulomb, viscous and static friction. (b): Stribeck friction model.

1.1.1 The Coulomb, the viscous and the Stribeck model

The most basic friction model is the Coulomb model [20] where the force of friction is given by

$$F_c = \mu F_n \operatorname{sign}(v) \tag{1.1}$$

where F_n is the normal force, μ the friction coefficient and v the relative velocity of the moving object. This is schematically represented in figure 1.2.

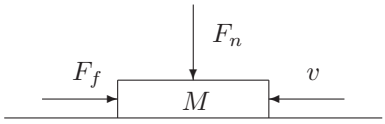

Figure 1.2: Schematic representation of the friction force F_f on an object M moving relative to a flat surface.

The viscous friction force is linear with respect to the velocity and can be expressed as

$$F_v(v) = \sigma_v v \tag{1.2}$$

with σ_v the viscous friction coefficient. The Stribeck effect can be expressed as a describing function of velocity and is kept here in the general form $F_s(v)$. The total friction force including all three effects can be expressed as

$$F_f(v) = \mu F_n \operatorname{sign}(v) + \sigma_v v + F_s(v) \tag{1.3}$$

1.1.2 Switching models

The basic friction models discussed in the previous section describe the friction forces well for steady-state velocities. For velocities in the area where $v = 0$ and for situations where the velocity crosses the $v = 0$ line, the models give numerical problems. To overcome these numerical problems during simulations Karnopp [25] proposed to set the friction force equal to the force acting on the object, for a small neighborhood of zero velocity. Outside a defined neighborhood, friction is a function of velocity. Later on, this model turned out to suffer from numerical instabilities as well. Leine *et al.* [29] came up with a switch friction model to overcome these problems. It consists of three different sets of ordinary differential equations for the description in the stick, slip and the transition phase. Although it solved the numerical problems, it still lacked the ability to describe friction well enough for an accurate model with the elastic part specifically. In the next section the seven parameter model is discussed which further enhance these models into a more complete model.

1.1.3 The seven parameter model

The seven parameter model [4, 21] includes presliding displacement, Coulomb and viscous friction and the Stribeck curve with frictional lag. It consists of two separate

models, one for the stiction phase and one for the sliding phase. For the stiction phase the friction is simply modeled as a spring:

$$F_f(x) = \sigma_0 x \tag{1.4}$$

with σ_0 as the micro stiffness and x the displacement of the object subjected to the friction force.

In the sliding phase the friction is modeled as

$$F_f(\dot{x}, t) = \left(F_c + F_v|\dot{x}| + F_s(\gamma, t_2) \frac{1}{1 + \left(\frac{\dot{x}(t-\tau_L)}{\dot{x}_s} \right)^2} \right) \text{sign}(\dot{x}) \tag{1.5}$$

with

$$F_s(\gamma, t_2) = F_{s,a} + (F_{s,\infty} - F_{s,a}) \frac{t_2}{t_2 + \gamma} \tag{1.6}$$

with:

F_f	the friction force
F_c	the Coulomb friction force
F_v	the viscous friction force
F_s	the magnitude of the Stribeck friction
$F_{s,a}$	the magnitude of the Stribeck friction at the end of the previous sliding period
$F_{s,\infty}$	the magnitude of the Stribeck friction after a long time at rest (with a slow application of force)
σ_0	the tangential stiffness of the static contact
$\dot{x}_s$	the characteristic velocity of the Stribeck friction
τ_L	the time constant of frictional memory
γ	the temporal parameter of the rising static static friction
t_2	the dwell time, time at zero velocity

Equation (1.5) clearly shows that the model consists of the Coulomb (F_c), viscous (F_v) and Stribeck (F_s) friction with frictional memory. With this model an attempt is done to capture the dynamics of friction by introducing a time delay. This time delay only affects the friction in sliding phase and oversimplifies it. Furthermore the true friction-phenomena (which will be discussed later on in this report) observed in the presliding phase, are not captured by equation (1.4) for the stiction phase. Since there is no clear distinction between the presliding regime and the sliding regime, the transition between the two equations is not obvious. As a result the model fails to describe the transition behavior between the presliding and the sliding regime.

1.2 The Dahl model

Dahl [11] explained frictional behavior with an analogy for the stress-strain property for materials. For objects subjected to small displacements he observed that the objects returned to its original position. Dahl compared this with the spring-like elastic material behavior, occurring in the bonding forces between the two surfaces.

For larger displacements the bonding interface would undergo a plastic deformation resulting in a permanent displacement. The maximum stress that can be attained in the stress-strain characteristic resembles the stiction force. For ductile materials the maximum stress will decline for increasing strain before rupture takes place. That last point resembles the Coulomb friction in Dahl's comparison. In other words Dahl assumed that friction force is not only a function of the velocity but of displacement as well. The following empirical expression was found [12]:

$$\frac{dF_f(x)}{dx} = \sigma \left| 1 - \frac{F_f}{F_c} \operatorname{sign}(\dot{x}) \right|^n \operatorname{sign}\left(1 - \frac{F_f}{F_c} \operatorname{sign}(\dot{x}) \right) \tag{1.7}$$

With σ the stiffness parameter at equilibrium point $F_f = 0$ [N], F_c Coulomb friction, n is a material dependent parameter which is $0 \leq n \leq 1$ for brittle materials and $n \geq 1$ is for more ductile like materials. For the simplest case where $n = 1$ the stabilizing factor $\operatorname{sign}\left(1 - \frac{F_f}{F_c} \operatorname{sign}(\dot{x})\right)$ from the last part in equation (1.7) can be put equal to 1 according to Dahl, which results in:

$$\frac{dF_f}{dx} = \sigma \left(1 - \frac{F_f}{F_c} \operatorname{sign}(\dot{x}) \right) \tag{1.8}$$

Which can be written as the following time derivative:

$$\frac{dF_f}{dt} = \frac{dF_f}{dx} \cdot \frac{dx}{dt} = \sigma \dot{x} - \frac{F_f}{F_c} \sigma |\dot{x}| \tag{1.9}$$

With this expression Dahl is able to model predisplacement and hysteresis (figure 1.3 (a)) in a dynamic model but it is unable to capture many other phenomena like the Stribeck effect and the ability to predict stick-slip motion. Although it represents only an approximation of the presliding behavior, it formed the basis for more advanced models.

1.3 The LuGre model

The Dahl model forms the basis of the LuGre model [10] which can be shown with the introduction of $z = F_f/\sigma_0$ as a state variable. With equation (1.9) the Dahl model can be rewritten as

$$\frac{dz}{dt} = \frac{1}{\sigma_0} \frac{dF_f}{dx} \frac{dx}{dt} = \frac{1}{\sigma_0} \frac{dF_f}{dx} v = v - \sigma_0 \frac{|v|}{F_c} z \tag{1.10}$$

The LuGre model replaces the constant F_c with a velocity-dependent function $g(v)$ and adds two more terms. It has an additional damping σ_1 associated with microdisplacement and a memoryless velocity-dependent term $f(v)$ and results in:

$$\dot{z} = v - \sigma_0 \frac{|v|}{g(v)} z = v - h(v) z \tag{1.11}$$

$$F_f = \sigma_0 z + \sigma_1 \dot{z} + f(v) \tag{1.12}$$

with F_f the friction force, v the velocity between the two surfaces in contact and z the internal friction state.

In continuation of Dahl's comparison with strain, z can be interpreted as the average bristle deflection. The LuGre model represents a spring-like behavior for small displacements just like the Dahl model with σ_0 as the stiffness. σ_1 is the microdamping and $f(v)$ representing the macrodamping which normally stands for the viscous friction ($f(v) = \sigma_2 v$). For slow nanoscale-motion applications σ_1 is an important parameter for accurate predictions. For other systems with millimeter accuracies σ_1 will have a less important role. For systems with asymmetry in friction it is worthwhile to mention that different values for the parameters can be chosen for positive and negative values of velocity. Another advantage of the LuGre is that both the presliding and the sliding regimes are described by the same model. Rice and Ruina [31] and Bliman and Sorin also introduced dynamical models but compared to the LuGre model it contained less friction phenomena [15].

1.3.1 Zero-slip displacement

One of the properties of the LuGre model is the zero-slip displacement which in the literature is also known as position drift or plastic sliding. It basically comes down to the effect that after applying and releasing a force less than the stiction force the system does not return to its original position. After applying the force the system reacts initially as a spring and the mass moves a small distance till it is at steady-state. Similarly the state z builds up till steady-state is reached. After removing the force the state z returns to zero but the mass does not fully return. The elastoplastic friction model [14] provided a modification that solved this position-drift issue with the LuGre model. Although this model further improved the accuracy, it still lacked an other friction phenomena, called hysteresis with nonlocal memory, which is discussed next.

1.3.2 Rate dependency

Rate dependency can be shown in the presliding regime where the inertial forces can be neglected. For systems with hysteresis that are rate independent like the Dahl-model, every point of the velocity reversal is recovered in the force-position plane (see figure 1.3 (a)) once the force resumes the corresponding value, independently of the number of velocity reversals. This is called reversal point memory or the nonlocal memory. Since the LuGre model is rate dependent [5], as figure 1.3 (b) shows, it does not capture the reversal point memory (see figure 1.4). The rate dependency in LuGre is caused by the $g(v)$ term in equation (1.11) which captures the Stribeck effect.

1.4 The Leuven integrated friction model structure

The intergrated friction model structure [33], also known as the Leuven model, further improves the LuGre model by including presliding hysteresis with nonlocal memory. This type of hysteresis occurs for nonperiodic presliding and is an improvement for the model's accuracy with respect to reality. The model is captured by two equation just like the LuGre model. It consists of a friction force equation and a state equation. Again the state variable z represents the average deformation

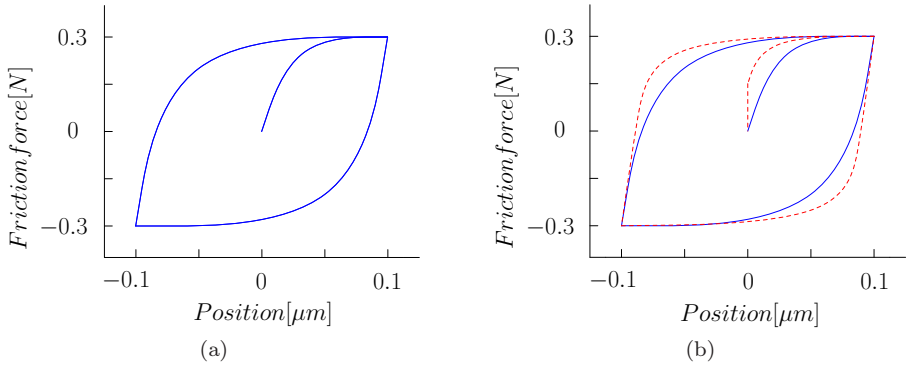

Figure 1.3: Behavior of the (a) Dahl and (b) LuGre models for sinusoidal inputs with two different frequencies.

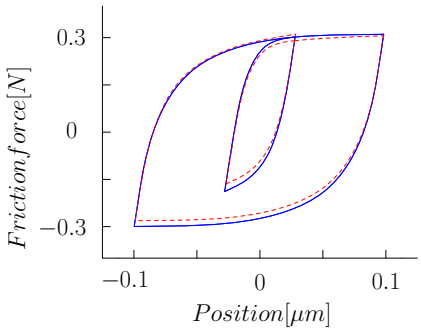

Figure 1.4: A qualitative comparison between the predicted behavior of the LuGre model (dashed line) and reality (solid line) at velocity reversals. The figure shows that the LuGre modeled hysteresis does not capture the nonlocal memory.

of the asperities of the contacting surfaces. The friction force and state equation are stated as:

$$F_f = F_h(z) + \sigma_1 \frac{dz}{dt} + \sigma_2 v \tag{1.13}$$

$$\frac{dz}{dt} = v\left(1 - \text{sign}\left(\frac{F_d(z)}{S(v) - F_b}\right) \cdot \left|\frac{F_d(z)}{S(v) - F_b}\right|^n\right) \tag{1.14}$$

with

σ_1	the micro-viscous damping coefficient
σ_2	the viscous damping coefficient
v	the velocity of the object
$F_h(z)$	the hysteresis friction force explained below
n	a coefficient determining the transition curve shape
$S(v)$	a function that models the constant velocity behavior given by:

$$S(v) = \text{sign}(v)\left(F_c + (F_s - F_c)e^{-(|v|/v_s)^\delta}\right) \tag{1.15}$$

1.4.1 The hysteresis function with nonlocal memory and the downside

The hysteresis friction force, represented by $F_h(z)$, consists of two parts and is shown in equation (1.16). At the beginning of a transition curve this is equal to F_b. The transition curve which is active at a certain time is called the current transition curve and is represented by $F_d(z)$.

$$F_h(z) = F_b + F_d(z) \tag{1.16}$$

The implementation for this hysteresis model requires two memory stacks for the non-local memory concept. One memory stack is needed for the minima of F_h and one for the maxima. At a velocity reversal one value is added to these stacks while one value is removed when closing an internal hysteresis loop. The stacks reset when the system goes from presliding to sliding. This mechanism requires that the state variable z resets to zero at each velocity reversal and is recalculated at the closing of an internal loop.
Although the Leuven model is a great improvement with respect to the nonlocal memory hysteresis, it also introduces a number of implementation difficulties and a discontinuity in the friction force for some circumstances. The implementation of the hysteresis function make some detections necessary for its mechanics to work. Each velocity reversal and velocity direction have to be detected so that the new values for F_b can be determined at the right moment. Another necessary check at every moment is the possible closing an inner hysteresis loop. An implementation error might occur when the memory stacks overflow when too many loops are initiated. This is possible because the stack size has to be chosen in advance. Furthermore a clear distinction has to be made between stick and sliding phase since the mechanic needs to reset the memory stacks at this point. Beside making the distinction, the transition between stick and sliding has to be detected as well. And the discontinuity in the friction force can occur when closing an inner hysteresis-loop without velocity reversal where the state variable z is reset to zero. To overcome these problems two adaptations to this model are discussed next.

1.4.2 The modified Leuven integrated friction model structure

The first modification in the Leuven model as presented in [26] is the adaptation of the state equation to solve the discontinuity issue discussed earlier. By replacing the argument $F_d(z)/(S(v) - F_b(z))$ in (1.14) with $F_h(z)/S(v)$ the new state equation becomes

$$\frac{dz}{dt} = v\left(1 - \text{sign}\left(\frac{F_h(z)}{S(v)}\right) \cdot \left|\frac{F_h(z)}{S(v)}\right|^n\right) \tag{1.17}$$

This modification ensures the functions for dz/dt and F_f to be continuous.

The second modification includes the replacement of the hysteresis force function with the Maxwell slip model. This implementation solves the stack overflow problem and other possible difficulties as discussed in the previous part. The Maxwell slip model basically comes down to the superposition of N elasto-slide elements representing the hysteresis force. In figure 1.5 the Maxwell slip model is schematically represented to illustrate this idea. This simplified representation into a finite

amount of elements is directly related to a disadvantage that results in a piece-wise approximation of the hysteresis function. The new hysteresis force function is stated as

$$F_h(k) = \sum_{i=1}^{N} F_i \tag{1.18}$$

where

$$F_i = K_i(z - \zeta_i) \tag{1.19}$$

for $|z - \zeta_i| < \frac{W_i}{k_i}$ and else

$$F_i = \text{sign}(z - \zeta_i)W_i \tag{1.20}$$

with

k_i	a linear spring-constant
ζ_i	the element position
W_i	the maximum force

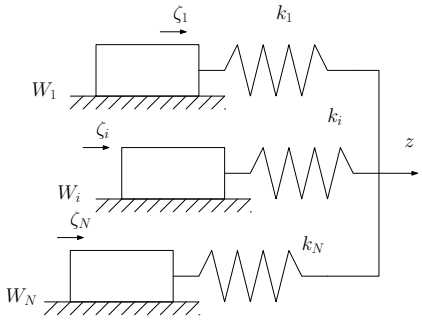

Figure 1.5: Global representation of the Maxwell slip friction model with N massless elements.

1.5 Physics-motivated friction models

The models described so far are all empirical based models. An other branch of friction models is the so called physics-motivated friction models. These describe friction on three different physical levels namely on atomic-molecular, asperity-scale and at tectonic-plate level. The asperity-scale level is the most common level for control purposes. In the literature many different physics based friction models can be found which all show strong similarities until a certain extension. The generic friction model (GFM) developed by Swevers *et al.* [1] will be used here as an example. Simulations normally consist of a large amount of asperities to acquire a decent representation. One asperity is shown in figure 1.6. The asperity has a lumped mass in the tip and is connected to the object with three springs. Due the nature of these models, more mechanisms can be taken into account compared to the empirical models such as normal creep, adhesion and impact of asperity masses for example. Haessig and Friedland [19] imagined asperities matching to bristles of a brush and called it the bristle model. Other closely related models are the Frenkel-Kontorova model [8, 18], the Tomlinson model, the Frenkel-Kontorova-Tomlinson model [35], the Burridge-Knopoff model [3] and the Tomlinson-Prandtl

atomic model. Although the physics-based models are capable of capturing all friction-induced phenomena that are observed so far, they are much too complicated for online control purposes. For this reason these models are not discussed here in further detail. Still it is worth mentioning these models in this study since these are used in the derivation of other models. One of these models, for control purposes specifically, is discussed next.

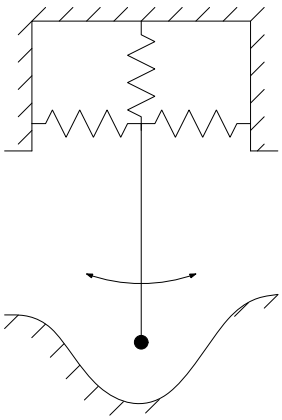

Figure 1.6: The generic friction model represented by one asperity.

1.6 The generalized Maxwell slip model

The generalized Maxwell slip model (GMS) [2] is a further development of the modified Leuven model as discussed in section 1.4.2. In the Maxwell slip model for hysteresis function of the modified Leuven model, the Coulomb law at slip is replaced by a rate-state law. This transforms the single state model modified Leuven into a multi state model for the GMS.
The friction force of the GMS model is expressed as

$$F_f(t) = \sum_{i=1}^{N}(k_i z_i(t) + \sigma_i \dot{z}_i(t)) + f(v) \tag{1.21}$$

with

z_i	the spring deflection
k_i	the spring stiffness
σ_i	the viscoelastic stiffness
$f(v)$	the viscous component

The dynamics of the elements are determined as follows. When the element sticks, the state equation is

$$\frac{dz_i}{dt} = v \tag{1.22}$$

and sticks until $z_i = s_i(v)$.
When the element slips, the state equation is

$$\frac{dz_i}{dt} = \text{sign}(v) C_i \left(1 - \frac{z_i}{s_i(v)}\right) \tag{1.23}$$

and remains slipping until the velocity passes through zero. $s_i(v)$ is the velocity-weakening Stribeck function for the ith element which can be described by three different parameters [3]. C_i is the attraction parameter, which determines how fast z_i converges to s_i. This results in a model consisting of six parameters per element. This number can be reduced with additional technics to two parameters per element and five extra parameters for the whole system. The GMS model behavior is compared in [27] with LuGre, Leuven and the GFM model. The GMS model proved to be the only model that is qualitative consistent with the GFM model for all properties with the nondrifting property in particular.

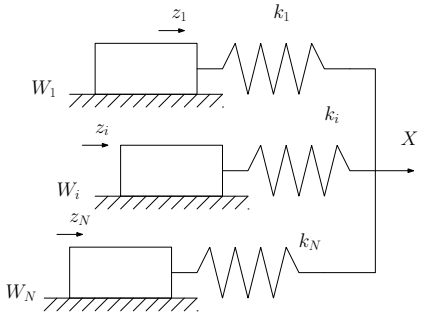

Figure 1.7: Global representation of the Maxwell slip friction model with N massless elements with z_i the position for each element.

Chapter 2

Friction compensation

For friction compensation numerous applications and variations can be found in literature which are partly summarized in [4]. These ways of compensation can be divided into model based and non-model based friction compensation and are discussed next into more detail.

2.1 Non-model based friction compensation

Examples of non-model based friction compensations are classic PD and PID feedback controllers, impulsive control and dither. Although the position tracking with a PD control is stable, stick-slip might occur at low velocity. This effect can be eliminated through high derivative, high proportional feedback or a combination of both but at cost of possible instability and the need for a strong actuator. An other issue is the steady-state tracking error which can be solved with integral control. Integral control on the other hand can cause limit cycling at low or zero velocity and can cause other difficulties at velocity reversals. These issues can be handled with a deadband and anti-windup at velocity reversal. But unfortunately these methods also introduce new issues like steady-state errors and decreasing performance.
Impulsive control achieves precise tracking by applying series of small impacts. This makes combinations of other technologies possible as well. For example the use of the impulsive control to achieve a controlled breakaway after which an other controller takes over to regulate the macroscopic movements.
Dither is a high frequency signal introduced into a system to modify its behavior which can result into a stabilizing effect. The focus here is the capability to smooth the discontinuity of friction at low velocity. After this application other friction compensation can be applied on top of this as would be done normally for the velocity dependent friction part.
For repetitive trajectories the iterative learning controller can be applied into a feedforward approach in order to compensate for friction and other undesired effects.
Another class of non-model based friction compensators are friction estimators. Examples of these are the Kalman-based filter, a predictive filter and a local function estimator which are compared in [30]. The Kalman-based method uses a random walk model that treats friction as a random constant and which should not be confused with the structured friction models used in model based observers. Many more non-model friction compensations are possible but are not further discussed

since the main focus in this study is model based friction compensation which is discussed next.

2.2 Model based friction compensation

Model based ways to compensate friction can be subdivided into feedforward and feedback approaches. The feedback compensation uses the real-time sensed system output while the feedforward compensation operates with a desired reference. Both systems can be expanded with adaption mechanisms to cope with changing model-parameters due to varying circumstances. The different control setups and variations found in literature are discussed in the next sections.

2.2.1 Feedback and feedforward friction compensation compared

The most basic form of feedforward is shown in figure 2.1. The feedback controller secures stability and increases disturbance rejection. The feedforward controller improves tracking performance in case of motion systems.

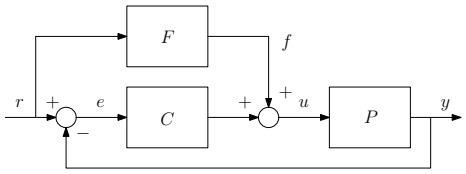

Figure 2.1: Schematic block diagram of elementary feedback control and feedforward.

Figure 2.1 shows plant P, feedback controller C and feedforward controller F. The signals shown are the reference trajectory r, servo error e, plant input u, plant output y and feedforward signal f. The overall transfer function is given by:

$$T_o = \frac{y}{r} = \frac{FP + CP}{1 + CP} \tag{2.1}$$

To acquire perfect tracking a suitable F is needed such that $T_o = 1$. This yields

$$FP + CP = 1 + CP \tag{2.2}$$

so that

$$F = P^{-1} \tag{2.3}$$

In [6] the feedforward controller consists of an acceleration feedforward part to compensate for the inertia forces and an inverse dynamic model. In practise however uncertainties and unmodelled and non-minimum phase dynamics make this difficult to implement. An other variation of this feedforward control is discussed in [7] where the feedforward is expressed as a prefilter R of the reference trajectory r with

$$R = 1 + \frac{F}{C} \tag{2.4}$$

and is used in combination with a non-causal filter. The effect of the pre-filter R is identical to the feedforward controller F. Some useful design tools however disappear and online tuning can be more complicated but in some cases more design freedom becomes available. This is not further discussed here in detail since the focus here is specifically for friction compensation.
Friction feedforward compensation precalculates the friction based on the desired reference trajectory which does not require an additional real-time closed loop calculation. In contrast to feedback, feedforward will not effect the closed loop stability. Before friction feedback compensation can be applied, a closed loop stability analysis must be performed to guarantee stability where sensor noise plays a role as well. The feedforward method is however limited by the use of the reference. The advantage of the feedback compensation is that it uses the actual state, or more precise the measured state, to calculate the friction compensation. The downside from this is that for the use of dynamic friction models the internal state cannot be measured. Internal state observers are necessary for those applications.
Both feedforward and feedback are compared in [24] for friction compensation. The used friction model here consists of the Karnopp model with viscous friction added. This static model only requires the velocity as input for both feedforward and feedback friction compensation. An important distinction is made here between the feedforward controller which provides accurate reference tracking and the feedback controller which tries to reject disturbances. The term disturbances covers disturbances caused by external loads and unmodeled dynamics in this case. The feedback controller should not be confused here with the feedback friction compensation which has a similar function to the feedforward friction compensation. First the model parameters are identified iteratively with the use of the feedback error-signal. By adjusting the feedforward parameters the uncompensated dynamics are successively extracted from the feedback errors. This is done until no further improvement is possible. After the identification the friction model is used in an experiment with both the feedforward and the feedback friction compensation. Both implementations resulted in a similar improvement with respect to the position and velocity error compared to an uncompensated situation. The feedback friction compensation however, performed better for velocities near zero and for steady-state situations. Although this result is not further discussed in this paper, a plausible explanation is the used static friction model. Since this model is less accurate for velocities near zero, the expected error for the predicted friction force is relative large here. The friction feedback controller is able to adapt to this error since it uses the actual output in contrast to feedforward compensation.

2.3 Feedforward friction compensation applications

An interesting comparison is shown in [28] where the Dahl model, the LuGre model, the Leuven model and the GMS model are compared in a feedforward compensation. The experimental results, executed in the neighbourhood of pre-sliding, show that the GMS model preformed best. It is remarked that although the GMS model performed better, the computational cost and the complexity of the parameter identification are comparable. To further improve the results, an disturbance

observer is added. The results prove to be according to the expectations and show further improvements. Model-based friction feedforward and a disturbance observer appear to complement each other.
In [17] a similar approach as with Karnopp model is taken for friction compensation and used in a feedforward application. The used friction model is torque-based and includes a "dead-zone torque" to describe the friction torque for forces below the stiction torque.
In [23] the GMS model and a static friction model are successfully used in a feedforward compensation. The main control consists of of a cascade PI velocity feedback and P position feedback controller. To further improve the friction compensation an inverse-model-based disturbance observer is added. The experiments show comparable results for both models for a tracking velocity in mainly the sliding regime. When reducing the tracking velocity to a presliding dominant regime, the GMS model shows to be superior. In [22] the remaining periodic disturbance is further minimized by including an repetitive controller. The resulting control setup is shown as a block diagram in figure 2.2. In the next section a comparable control setup is discussed with the friction compensation in feedback but without the repetitive control and the disturbance observer.

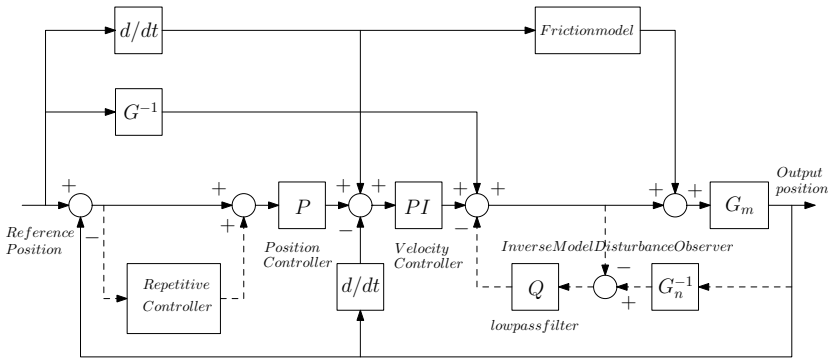

Figure 2.2: Schematic block diagram of cascade P/PI controller with friction feedforward, an inverse model based disturbance observer and a repetitive controller.

In [32] an adaptive static friction controller is presented based on sliding mode control. The coulomb and viscous friction are compensated with the adaptive feedforward control. The Stribeck and position dependent friction are compensated separately in a non-adaptive feedforward since these components are not linear in a parameter. The effectiveness is shown with numerical simulations.

2.4 Feedback friction compensation applications

In [13] the dynamical friction model LuGre is used in a feedback manner with the addition of a observer for the non-measurable internal friction state. The closed-loop stability analysis is performed similarly as discussed in [10] to guarantee stability. To cope with varying normal forces, the control is expanded with an adaptive

friction compensation similar to [9]. Other varying circumstances like humidity and temperature can be compensated as well with other adaptation mechanisms but are assumed to be constant for this setup. The adaptive friction compensation however did not show any improvements in the experimental results, possibly because friction is not the dominant disturbance for this system. The experimental results for feedback friction compensation compared to a feedforward form proved that the feedforward performed better in this study. A comparable adaptive friction compensation based on LuGre is presented in [36] where it is called ANDFC (adaptive nonlinear dynamic friction compensation). Instead of the measured velocity or electronic differentiation of the position, an estimation method is used to prevent large deviation in the estimated velocity.
In [34] a distinction is made between friction feedforward compensation and command feedforward. Command feedforward here compensates the servo lag phenomena with an acceleration and a velocity term. The friction feedforward described here is based on the Karnopp model fed with an estimated system-output velocity. The friction compensation is nested in a position feedback-loop so the term feedforward is somewhat misleading here and the term friction feedback would be more appropriate. A block diagram of the multi-loop system is shown in figure 2.3.

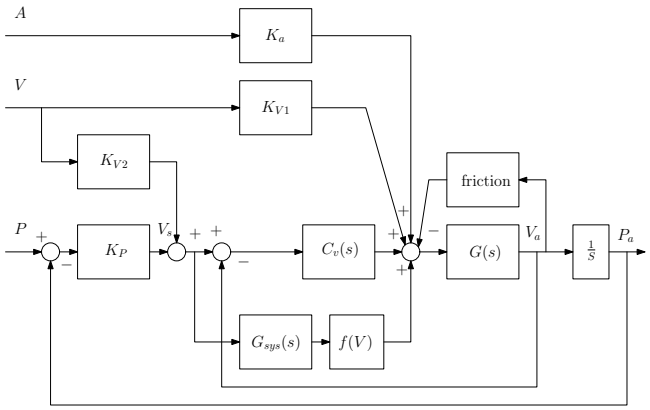

Figure 2.3: Block diagram of a cascade control system with friction compensation in feedback.

In this figure P, V and A are the commanded position and the related velocity and acceleration respectively. V_s, P_a and V_a are the commanded velocity and the actual output position and velocity. K_P and $C_V(s)$ are the position and velocity controllers respectively. K_a, K_{v1} and K_{v2} are feedforward parameters and $f(V)$ represents the friction model. $G_{sys}(s)$ is the following transfer function

$$G_{sys}(s) = \frac{C_V(s)G(s)}{1 + C_V(s)G(s)} \tag{2.5}$$

Although the experimental results showed an improvement compared to the situation without friction compensation, the results heavily depend on the accuracy of the modeled plant $G(s)$ in equation (2.5). Although the friction compensation is

considered to be in a feedforward formulation in this paper, stability still has to be proved here since the friction compensation is nested in a feedback loop. An other comment about this interesting setup is that neither the reference nor the output signal is directly used to determine the friction force. Instead the signal between the position controller and velocity controller is used to calculate the modeled system output so that at last a friction estimation can be made. In general it can be said that this setup for friction compensation is indirect, complex and dependent on the accuracy of the modeled system. It remains unclear if the presented control setup offers any advantages compared to other friction compensation strategies. In [16] an alternative method to identify the frictional behavior with the help of an iterative learning controller (ILC) is discussed. From the learned feedforward signal for different constant velocities, the friction model parameters, the position dependent friction and the cogging are identified. Static friction is identified separately with break-away experiments. The resulting friction model is implemented in a feedback compensation. In this report the static friction model Tustin is used since the position sensor in this application is not accurate enough to identify presliding and frictional lag. Other phenomena that occur are found dominant so this simplification is considered justified.

Chapter 3

Conclusion

Different friction models and applications are discussed in this study and compared. Literature shows that dynamic friction models are able to predict friction more accurately than static friction models. Although performing better, dynamic models require a more complex model with more parameters. This makes it generally more difficult to implement and identify and increases the online computational costs. Whether or not a dynamical friction compensation is useful to implement fully depends on the applied system and requirements on accuracy. Systems operating mainly in the sliding regime will benefit less from a dynamical friction compensation compared to a system operating at low velocity or where velocity reversals occur often. The measured system-output should be accurate enough in order to be able to identify the dynamic friction phenomena before dynamic friction compensation becomes useful. For systems where friction is not the dominating disturbing factor, other control efforts should be considered first.
In chapter 1 different friction models found in literature are discussed. The Coulomb, the viscous and the Stribeck model are discussed first which form the basic elements of friction. Numerical problems caused by the discontinuity at zero velocity are solved with Switching models. The last static model discussed is the seven parameter model which attempts to include the frictional lag. The model consists of a separate model for the presliding phase and a model for the sliding phase. However, the transition between the phases is not well described. In the Dahl model, the friction is not only a function of velocity but of displacement as well. With the Dahl model predisplacement and hysteresis can be captured but it still lacks other friction phenomena. The LuGre model continued this dynamical model into a single model suitable for both presliding and sliding regime and the transition between them. Although the LuGre model is able to capture almost all known friction phenomena it still lacks the ability to describe hysteresis with nonlocal memory and undesired position drift occurred in simulation. These issue's are solved in the Leuven model, but at the cost of numerical and implementation problems. With two modifications a discontinuity issue and the implementation problem are solved in the modified Leuven model. Finally physics-motivated friction models are briefly discussed to introduce the generalized maxwell slip model. This model contains several internal states z instead of one which allows to describe the presliding behavior even more accurate.
To further improve accuracy, friction compensation is normally applied combined with other control methods. These commonly consist of a feedback control to reject

disturbances and an inertia feedforward for motion systems. Besides these basic techniques a vast number of other techniques are possible. The idea of combining these different controllers is that they complement each other and result in further improvement and adaptation to changing circumstances. Chapter 2 discusses these different control technics which are divided into model based and non-model based friction compensation. First the non-model based friction compensations are discussed where the classic feedback control, impulsive control, dither, ILC and friction estimators are considered in this review. Next, model based friction compensations are subdivided into feedforward and feedback approaches and discussed. First the global differences for feedforward and feedback are discussed and the experimental results of both methods are compared for a static friction model. Different applications for feedforward compensation are discussed next. First different dynamical friction models and static model are compared. Next an application of the GMS model is discussed which is applied with a cascade position/velocity feedback controller together with an inertia feedforward, a repetitive controller and an inverse model disturbance observer to further minimize the tracking error. And at last a friction controller based on sliding mode control is discussed shortly. Next, different feedback friction compensation applications are discussed. The implementation of the LuGre model with a state observer is discussed with an additional adaptation mechanism to cope with varying circumstances. Then an application with a static friction model nested in a feedback-loop is discussed where the model is fed with a modeled plant output. And at last, a report is discussed where the ILC is used to identify the friction model-parameters which is than used in a feedback configuration.

Bibliography

[1] F. Al-Bender, V. Lampaert, and J. Swevers. A novel generic model at asperity level for dry friction force dynamics. *Tribology Letters*, 16(1-2):81–94, 2004.

[2] F. Al-Bender, V. Lampaert, and J. Swevers. The generalized maxwell-slip model: A novel model for friction simulation and compensation. *IEEE Transactions on Automatic Control*, 50(11):1883–1887, 2005.

[3] F. Al-Bender and J. Swevers. Characterization of friction force dynamics. *IEEE Control Systems Magazine*, 28(6):64–81, 2008.

[4] B. Armstrong-H'elouvry, P. Dupont, and C. Canudas de Wit. A survey of models, analysis tools and compensation methods for the control of machines with friction. *Automatica*, 30:1083–1138, 1994.

[5] K.J. Åström and C. Canudas-de-Wit. Revisiting the lugre friction model. *IEEE Control Systems Magazine*, 28(6):101–114, 2008.

[6] M. Boerlage, M. Steinbuch, P. Lambrechts, and M. Van De Wal. Model-based feedforward for motion systems. volume 2, pages 1158–1163, 2003.

[7] M. Boerlage, R. Tousain, and M. Steinbuch. Jerk derivative feedforward control for motion systems. volume 5, pages 4843–4848, 2004.

[8] O.M. Braun and Y.S. Kivshar. Nonlinear dynamics of the frenkel-kontorova model. *Physics Report*, 306(1-2):1–108, 1998.

[9] C. Canudas De Wit and P. Lischinsky. Adaptive friction compensation with partially known dynamic friction model. *International Journal of Adaptive Control and Signal Processing*, 11(1):65–80, 1997.

[10] C. Canudas de Wit, H. Olsson, K.J. Astrom, and P. Lischinsky. New model for control of systems with friction. *IEEE Transactions on Automatic Control*, 40(3):419–425, 1995.

[11] P.R. Dahl. A solid friction model. *The Aerospace Corporation. Technical report*, 1968.

[12] P.R. Dahl. Measurement of solid friction parameters of ball bearings. *The Aerospace Corporation. Technical report*, 1977.

[13] N.J.M. van Dijk. Adaptive friction compensation of an inertia supported by mos2 solid-lubricated bearings. Technical report, Eindhoven University of technology, Eindhoven, The Netherlands, 2005.

[14] P. Dupont, V. Hayward, B. Armstrong, and F. Altpeter. Single state elastoplastic friction models. *IEEE Transactions on Automatic Control*, 47(5):787–792, 2002.

[15] M. Gafvert. Comparisons of two dynamic friction models. pages 386–391, 1997.

[16] J.A. van Geenhuizen. Friction compensation for the printer system. Master's thesis, Dept. Mech. Eng., Eindhoven Univ. Technol., Eindhoven, The Netherlands, 2008.

[17] Julio J. Gonzalez and Glenn R. Widmann. A new model for nonlinear friction compensation in the force control of robot manipulators. pages 201–203, 1997.

[18] Y. Guo, Z. Qu, Y. Braiman, Z. Zhang, and J. Barhen. Nanotribology and nanoscale friction. *IEEE Control Systems Magazine*, 28(6):92–100, 2008.

[19] Jr. D.A. Haessig and B. Friedland. On the modeling and simulation of friction. *Journal of Dynamic Systems, Measurement and Control, Transactions of the ASME*, 113(3):354–362, 1991.

[20] A. Harnoy, B. Friedland, and S. Cohn. Modeling and measuring friction effects. *IEEE Control Systems Magazine*, 28(6):82–91, 2008.

[21] R.H.A. Hensen. *Controlled mechanical systems with friction*. PhD thesis, Dept. Mech. Eng., Eindhoven Univ. Technol., Eindhoven, The Netherlands, 2002.

[22] Z. Jamaludin, H. van Brussel, G. Pipeleers, and J. Swevers. Accurate motion control of xy high-speed linear drives using friction model feedforward and cutting forces estimation. *CIRP Annals - Manufacturing Technology*, 57(1):403–406, 2008.

[23] Z. Jamaludin, H. van Brussel, and J. Swevers. Quadrant glitch compensation using friction model-based feedforward and an inverse-model-based disturbance observer. *Advanced Motion Control, 2008. AMC '08. 10th IEEE International Workshop on*, pages 212 – 217, 2008.

[24] C.T. Johnson and R.D. Lorenz. Experimental identification of friction and its compensation in precise, position controlled mechanisms. *IEEE Transactions on Industry Applications*, 28(6):1392–1398, 1992.

[25] D. Karnopp. Computer simulation of stick-slip friction in mechanical dynamic systems. *Journal of Dynamic Systems, Measurement and Control, Transactions of the ASME*, 107(1):100–103, 1985.

[26] V. Lampaert, J. Swevers, and F. Al-Bender. Modification of the leuven integrated friction model structure. *IEEE Transactions on Automatic Control*, 47(4):683–687, 2002.

[27] V. Lampaert, J. Swevers, and F. Al-Bender. A generalized maxwell-slip friction model appropriate for control purposes. *Proc. IEEE Int. Conf.Physics and Control*, pages 1170–1178, 2003.

[28] V. Lampaert, J. Swevers, and F. Al-Bender. Comparison of model and non-model based friction compensation techniques in the neighbourhood of pre-sliding friction. volume 2, pages 1121–1126, 2004.

[29] R.I. Leine, D.H. van Campen, A. de Kraker, and L. van den Steen. Stick-slip vibrations induced by alternate friction models. *Nonlinear Dynamics*, 16(1):41–54, 1998.

[30] A. Ramasubramanian and L.E. Ray. Stability and performance analysis for non-model-based friction estimators. volume 3, pages 2929–2935, 2001.

[31] J.R. Rice and A.L. Ruina. Stability of steady frictional slipping. *Journal of Applied Mechanics, Transactions ASME*, 50(2):343–349, 1983.

[32] G. Song, Y. Wang, L. Cai, and R.W. Longman. Sliding-mode based smooth adaptive robust controller for friction compensation. volume 5, pages 3531–3535, 1995.

[33] J. Swevers, F. Al-Bender, C.G. Ganseman, and T. Prajogo. An integrated friction model structure with improved presliding behavior for accurate friction compensation. *IEEE Transactions on Automatic Control*, 45(4):675–686, 2000.

[34] M.C. Tsai, I.F. Chiu, and M.Y. Cheng. Design and implementation of command and friction feedforward control for cnc motion controllers. *IEE Proceedings: Control Theory and Applications*, 151(1):13–20, 2004.

[35] M. Weiss and F.J. Elmer. Dry friction in the frenkel-kontorova-tomlinson model: Static properties. *Physical Review B - Condensed Matter and Materials Physics*, 53(11):7539–7549, 1996.

[36] Y. Zhang, G. Liu, and A.A. Goldenberg. Friction compensation with estimated velocity. volume 3, pages 2650–2655, 2002.